ISSN 1063-7850, Technical Physics Letters, 2015, Vol. 41, No. 5, pp. 418–421. © Pleiades Publishing, Ltd., 2015.
Original Russian Text © A.S. Elshin, N.Yu. Firsova, M.A. Marchenkova, V.I. Emel'yanov, I.P. Pronin, S.V. Senkevich, E.D. Mishina, A.S. Sigov, 2015, published in Pis'ma v Zhurnal Tekhnicheskoi Fiziki, 2015, Vol. 41, No. 9, pp. 16–23.

Nonlinear Optical Diagnostics of Local Crystallization of Lead Zirconate Titanate Films Using Femtosecond Laser Radiation

A. S. Elshin[a] *, N. Yu. Firsova[a], M. A. Marchenkova[a], V. I. Emel'yanov[b], I. P. Pronin[c], S. V. Senkevich[c], E. D. Mishina[a], and A. S. Sigov[a]

[a] *Moscow State Technical University of Radio Engineering, Electronics, and Automatics, Moscow, 119454 Russia*
[b] *Moscow State University, Moscow, 119991 Russia*
[c] *Ioffe Physical Technical Institute, Russian Academy of Sciences, St. Petersburg, 194021 Russia*
**e-mail: elshin_andrew@mail.ru*

Received October 7, 2014

Abstract—Features of crystallization of microstructures to the perovskite-like phase in a lead zirconate titanate film are studied using multiple near-IR femtosecond laser pulse radiation. The kinetics of crystallization is in situ investigated using the second-harmonic generation technique. It is established that the crystallization is divided into high-temperature ultrafast (explosive) crystallization, which occurs right after the start of irradiation, and low-temperature slow (self-induced) crystallization, which starts after termination of irradiation of a strained multilayer structure. The advantages of the second-harmonic generation microscopy in studying annealed microstructures are demonstrated.

DOI: 10.1134/S1063785015050041

Thin-film ferroelectric structures are the basis of a new generation of micro- and nanoelectronic devices [1, 2]. The transition of an amorphous film to the ferroelectric phase is ensured by annealing. In most techniques, thermal annealing in a furnace, including one with programmable temperature control, is used [3].

Laser annealing is applied for local crystallization of amorphous films to the ferroelectric phase to minimize heating of elements surrounding the functional area. Upon annealing by excimer lasers with a photon energy much higher than the band gap, absorption and, consequently, annealing occur in the thin surface layer [4]. In addition, the mode structure of a spot in excimer lasers does not allow localizing the annealing in the submicron region.

In study [5], we proposed annealing a ferroelectric film on a platinized substrate with the use of a single-mode femtosecond laser with wavelength falling into the film transparency region and, simultaneously, to the absorption region of platinum. This technique makes it possible to solve three problems at once. First, the annealing conditions can be made similar to those of thermal annealing in a furnace, since the film is heated from the side of platinum. Second, heating is performed locally with the Gaussian temperature distribution along the laser spot radius. Third, the femtosecond laser makes it possible to examine the formation of a ferroelectric phase during annealing. This diagnostics is based on the second optical harmonic generation (SHG), which is an effective technique for studying phase transitions, including crystallization to the perovskite phase.

This Letter presents new experimental time dependences of the SHG intensity in comparison with the data of the theoretical analysis of crystallization, which allows establishing the crystallization mechanism. It is shown that the SHG technique has advantages over the linear optical methods in ex situ visualization of annealed areas.

Films of the lead zirconate titanate (PZT) solid solution with a thickness of 700 nm and a 10% lead oxide excess ($Pb(Zr_{0.54}Ti_{0.46})O_3$ + 10 mol %PbO) were deposited onto a platinized silicon substrate by rf magnetron sputtering without annealing [6]. The substrate thickness was 300 μm, the silicon oxide layer thickness was 300 nm, and the platinum layer thickness was 80 nm. The effective heat removal from the multilayer system was ensured by a heat conducting contact attached to the substrate from below.

The laser radiation source used was an Avesta-Proekt femtosecond Ti:sapphire laser with a wavelength of 800 nm, a pulse length of 100 fs, and a pulse repetition rate of 100 MHz. The irradiation time upon annealing was 1–30 s. To focus the beam upon annealing and detect the SHG with a wavelength of 400 nm, a Witek Alpha-300 confocal microscope was used. A focusing objective ×40 with numerical aperture N_A = 0.65 formed a 1-μm laser spot on the film surface estimated as a waist width. At the in situ monitoring of annealing, scanning of a laser spot over the sample was

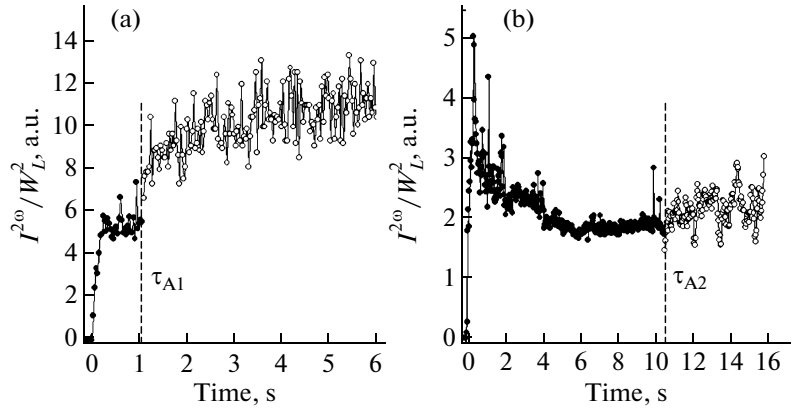

Fig. 1. Experimental time dependences of normalized SHG intensities during heating ($0 < t < \tau_A$) and cooling ($t > \tau_A$) at annealing beam power $W_A = 1$ MW/cm^2 and annealing times $\tau_{A1} = 1$ s and $\tau_{A2} = 10$ s.

not performed. A scheme with two parallel beams, annealing and diagnostic, was used. The density of power of the annealing beam was $W_A = 1.0$ MW/cm^2, and that of the diagnostic beam was $W_D = 0.2$ MW/cm^2. Annealing and its detection were carried out as follows: on the path of the annealing beam, a gate was placed, which was opened only for annealing time τ_A, whereas the diagnostic beam fell onto the sample and the SHG was detected over the whole experimental time. The gate opening moment, i.e., the start of annealing, was taken as time reference point $t = 0$. Thus, at $t < 0$, the SHG signal from the unannealed film was detected at laser power W_D; at $0 < t < \tau_A$, the SHG signal was detected during annealing at the resulting power of the annealing and diagnostic beams $W_A + W_D$, and at $t > \tau_A$, after shutting the gate, the SHG signal was detected during cooling-down/crystallization at laser power W_D. Since the SHG intensity is proportional to the squared incident power, the SHG signal was normalized to the corresponding squared power in each interval, $t < 0$, $0 < t < \tau_A$, and $t > \tau_A$, to compare the results for all the areas.

The results of annealing were controlled by ex situ confocal optical and nonlinear optical microscopy. Images were obtained by scanning a sample using a diagnostic beam with a wavelength of 800 nm and power density $W_D = 0.2$ MW/cm^2; in linear and SHG microscopy, radiation at respective wavelengths of 800 and 400 nm was detected.

Figure 1 shows normalized time dependences of the SHG intensity for annealing times τ_{A1} and τ_{A2}.

Before the commencement of irradiation, there is no SHG signal from the amorphous PZT film. After switching on the annealing radiation (time $t = 0$ in Fig. 1a), the PZT film is heated to about 700 K for a short time of about 0.1 s, which was found by the two-dimensional heat conduction equation using the COMSOL Multiphysics package due to the optical absorption in the Pt layer. At these times, ultrafast crystallization of a part of the film material occurs with the transition to the noncentrosymmetrical perovskite phase, which is accompanied by a sharp increase in the SHG signal. Such an ultrafast crystallization apparently follows not the classical nucleation mechanism, which works under the conditions of slow (in hours) furnace annealing [7], but ultrafast explosive PZT crystallization, or the order–disorder transition [8].

Then, the SHG intensity growth saturates and the SHG signal remains approximately the same for the whole irradiation time $\tau_{A1} = 1$ s. The SHG saturation can result from inhibition of the PZT crystallization due to the sharp growth of the crystallization activation energy because of large tensile stresses in the amorphous regions surrounding the crystallized areas [9]. Such stresses occur due to an increase in the density of the crystallized material (a decrease in its volume) as compared with the volume of the initial amorphous phase [6].

After switching off the annealing irradiation, i.e., at $t = \tau_A$ (Fig. 1a), the PZT film, including both the perovskite phase and the Pt layer, is sharply cooled to room temperature for times of no more than 0.1 s and, consequently, the film volume sharply decreases. Due to the larger coefficient of thermal expansion, the Pt layer is compressed more strongly, so the PZT film experiences impact compressive stress. We may assume that this impact reduction of the activation energy induces a slow explosive crystallization wave propagating to the PZT region from the perovskite phase areas. Investigation shows that the critical temperature of ignition and propagation of this wave [10] can be lower than room temperature due to the huge latent heat of PZT crystallization and a strain-induced decrease in the activation energy. Under these conditions, the crystallization wave (phase reversal wave) can propagate to the amorphous region at room temperature via release of the latent heat of crystallization at its front. This explains the presence of an area of a slow increase in the SHG signal after switching off the irradiation. The described effect is pronounced at short annealing time τ_{A1} (Fig. 1a).

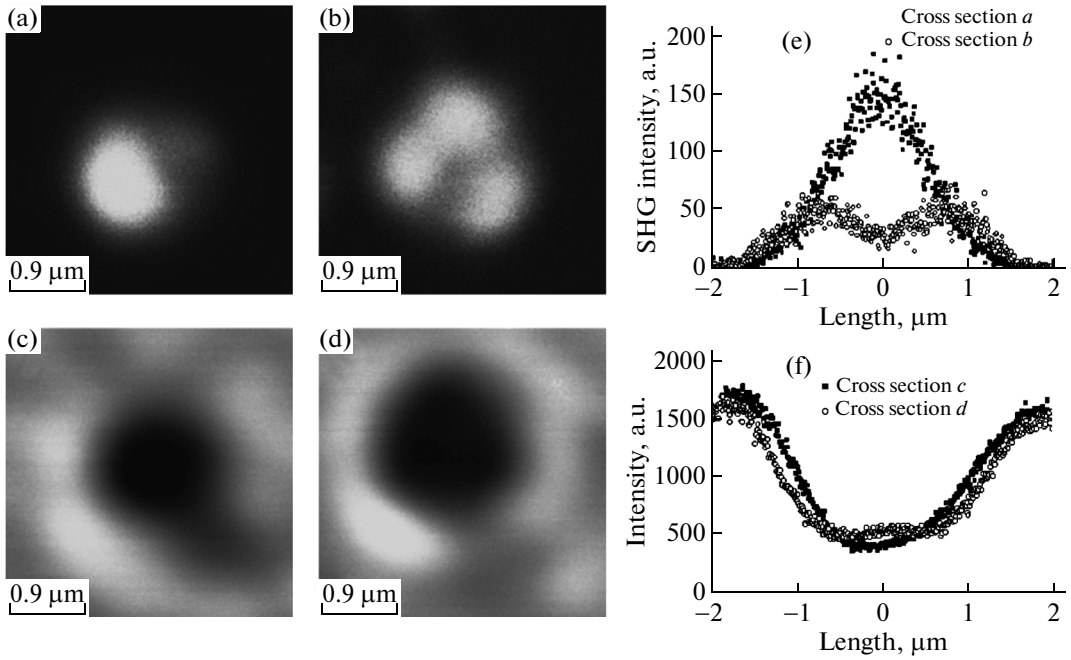

Fig. 2. (a, b, e) Nonlinear optical images of annealed regions (the incident radiation wavelength is 800 nm, while the detected SHG radiation wavelength is 400 nm) and their cross sections. (c, d, f) Linear optical images of annealed regions (the incident, while the detected radiation wavelength is 800 nm) and their cross sections. The annealing time is (a, c) 1 and (b, d) 10 s.

An increase in the annealing time to τ_{A2} (Fig. 1b) leads to a decrease in the SHG signal. A decrease in the SHG signal can be caused by the fact that at the spot center, where the temperature is maximum, the film can be fused with the formation of cracks and other defects. We may assume that the defects that form upon fusion damp the propagation of the crystallization wave.

The presence of the defect region at large annealing times is confirmed by SHG microscopy (Fig. 2). The nonlinear optical images upon annealing for times τ_{A1} and τ_{A2} are substantially different. At τ_{A1}, the region of annealing is a bright regular circle and the cross section is approximated by the Gaussian function with full width at half-maximum FWHM = 1.5 μm, which corresponds to the calculated size of the annealed region. At τ_{A2}, the region of annealing is a ring structure with a dark spot at the center, which can be seen in both the image and its cross section. A decrease in the SHG signal at the center of the annealed region is indicative of the perovskite structure break.

It should be emphasized that testing of annealed regions using ordinary (linear optical) microscopy does not resolve the cases of optimal and nonoptimal laser annealing. This can be seen in Figs. 2c and 2d. The linear images have the same circular, slightly distorted shape with the strongly spread edge region. The cross sections of the linear images built from the spot diameter are approximated by the Gaussian function and differ by only the FWHM value, which is 2 and 3 μm for τ_{A1} and τ_{A2}, respectively.

Thus, we have proposed a technique for local crystallization of perovskite microstructures in amorphous PZT film using femtosecond laser radiation with monitoring of the kinetics of crystallization by the intensity of the second optical harmonic. We managed to obtain a series of ferroelectric microstructures with a size of 1 μm. Study of these structures using atomic force microscopy in the piezoelectric mode confirmed the presence of ferroelectric polarization and showed the possibility of its switching. The second harmonic generation technique allowed us to elucidate the features of crystallization—specifically, its explosive character at the initial stage and the transition to the self-induced mode after finish of annealing. It was confirmed that, to obtain a microstructure with a smooth spatial profile of the perovskite phase, in addition to the narrow power density range that was found earlier [11], the time annealing interval is also narrow. An increase in the annealing time leads to the formation of ring perovskite structures with a defect center, which can be easily revealed by SHG microscopy. The proposed techniques significantly enhance the controllability of laser annealing and can be used not only in ferroelectrics, but also in a wide range of materials crystallizing in the noncentrosymmetrical phase.

Acknowledgments. This study was supported by the Ministry of Education and Science of the Russian Federation, state order no. 11.144.2014.

REFERENCES

1. K. A. Vorotilov, A. S. Sigov, A. A. Romanov, and P. R. Mashevich, Nanomater. Nanostruk., No. 1, 45 (2010).
2. Y. Shen and G. Z. Cao, Ferroelectrics **342**, 15 (2006).
3. A-D. Li, D. Wu, H.-Q. Ling, M. Wang, Zh. Liu, and N. Ming, J. Cryst. Growth **235**, 394 (2002).
4. D. N. Khmelenin, O. M. Zhigalina, K. A. Vorotilov, and I. G. Lebo, Phys. Solid State **54** (5), 999 (2012).
5. N. Yu. Firsova, E. D. Mishina, A. S. Sigov, S. V. Senkevich, I. P. Pronin, A. Kholkin, I. Bdikin, and Yu. I. Yuzyuk, Ferroelectric **433** (1), 164 (2012).
6. I. P. Pronin, E. Yu. Kaptelov, S. V. Senkevich, V. A. Klimov, N. V. Zaitseva, T. A. Shaplygina, V. P. Pronin, and S. A. Kukushkin, Phys. Solid State **52** (1), 132 (2010).
7. Z. Huang, Q. Zhang, and R. W. Whatmore, J. Appl. Phys. **85** (10), 7355 (1999).
8. H. Hu, C. J. Peng, and S. B. Krupanidhi, Thin Solid Films **223**, 327 (1993).
9. I. Yu. Tentilova, E. Yu. Kaptelov, I. P. Pronin, and V. L. Ugolokov, Inorg. Mater. **48** (11), 1136 (2012).
10. V. I. Emel'yanov and I. M. Panin, Appl. Phys. A **57**, 561 (1993).
11. N. Yu. Firsova, A. S. Elshin, M. A. Marchenkova, A. K. Bolotov, M. S. Ivanov, I. P. Pronin, S. V. Senkevich, D. A. Kiselev, and E. D. Mishina, J. Nano Microsyst. Tech. **7** (168), 43 (2014).

Translated by E. Bondareva